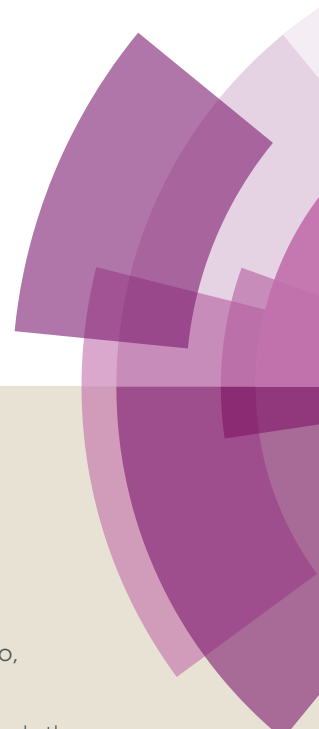


# Journal of Materials Chemistry C

Accepted Manuscript



This article can be cited before page numbers have been issued, to do this please use: P. C. Xue, B. Yao, Y. Shen and H. Gao, *J. Mater. Chem. C*, 2017, DOI: 10.1039/C7TC03752J.



This is an Accepted Manuscript, which has been through the Royal Society of Chemistry peer review process and has been accepted for publication.

Accepted Manuscripts are published online shortly after acceptance, before technical editing, formatting and proof reading. Using this free service, authors can make their results available to the community, in citable form, before we publish the edited article. We will replace this Accepted Manuscript with the edited and formatted Advance Article as soon as it is available.

You can find more information about Accepted Manuscripts in the [author guidelines](#).

Please note that technical editing may introduce minor changes to the text and/or graphics, which may alter content. The journal's standard [Terms & Conditions](#) and the ethical guidelines, outlined in our [author and reviewer resource centre](#), still apply. In no event shall the Royal Society of Chemistry be held responsible for any errors or omissions in this Accepted Manuscript or any consequences arising from the use of any information it contains.



Journal Name

ARTICLE

## Self-assembly of fluorescent galunamide derivative and sensing of acid vapor and mechanical force stimuli

Pengchong Xue,<sup>a,b,\*</sup> Boqi Yao<sup>b</sup> Yanbing Shen,<sup>b</sup> and Hongqiang Gao<sup>b</sup>Received 00th January 20xx,  
Accepted 00th January 20xx

DOI: 10.1039/x0xx00000x

www.rsc.org/

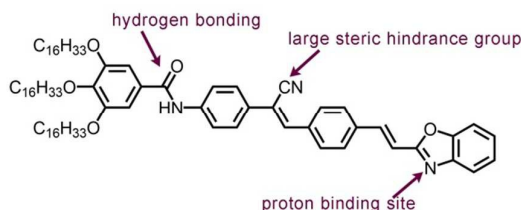
A galunamide derivative consisting of a fluorophore with benzoxazole and cyano unit was designed and synthesized to realize dual response to acid vapor and mechanical force. Photophysical properties and self-assembly were investigated. The dilute solution could respond to acid stimulus, and the emission peak at 472 nm shifted to 535 nm with the addition of trifluoroacetic acid (TFA). Moreover, the derivative could self-assemble into thin nanofibers in its gel phase, and the fluorescence of xerogel film is sensitive to TFA vapor. The emission color gradually changed from yellow to orange red upon exposure to acid vapor, and the detection limit is as low as 70 ppb for TFA. The solid exhibited reversible fluorescence color change under the stimuli of mechanical force and solvent annealing. The UV-vis absorption and IR spectra indicate that the fluorescence color conversion can be attributed to the destruction of intermolecular hydrogen bonds and pristine  $\pi$ - $\pi$  interaction induced by mechanical force.

### Introduction

Stimuli-responsive smart materials can change their chemical and physical properties under external stimuli, such as light, heat, anions, cations, mechanical force, various gases, magnetic field, and so on.<sup>1</sup> These stimuli sources may induce molecular structure or intermolecular interaction changes in materials. Among these materials, luminescent organic materials that respond to various stimuli sources have been widely developed.<sup>2</sup> External stimuli always induce these luminescent organic molecules to alter their emission intensity, emission wavelength, or luminescence lifetimes. Thus far, luminescent organic molecules act as sensor to detect ions in solution state<sup>3</sup> and quantitatively sense gases, such as organic amines,<sup>4</sup> O<sub>2</sub>,<sup>5</sup> CO<sub>2</sub>,<sup>6</sup> SO<sub>2</sub>,<sup>7</sup> HCl,<sup>8</sup> NH<sub>3</sub>,<sup>9</sup> trinitrotoluene,<sup>10</sup> and picric acid<sup>11</sup> in film state. For obtaining rapid response to gaseous analytes and low detection limits, large surface area is needed for sensing films.<sup>12</sup> 3D networks consisting of a large number of thin self-assemblies can be easily supported in supramolecular gels constructed by low molecular mass gelators.<sup>13</sup> Their xerogel film may provide large surface area and porous microstructure, which can enhance the adsorption and accumulation of gaseous molecules. Moreover, the strong

$\pi$ - $\pi$  interaction between luminescent gelator and long-range exciton migration within gel nanofibers can amplify fluorescence quenching with the help of surface-adsorbed analytes.<sup>14</sup> To date, several fluorescent or phosphorescent organogels have been developed for sensing gases, such as, O<sub>2</sub>,<sup>15</sup> organic amines,<sup>16</sup> volatile acids,<sup>17</sup> explosives<sup>18</sup> and humidity.<sup>19</sup>

Recently, luminescent materials in response to mechanical force have received significant attention because these materials can change luminescent color, intensity, or lifetime under external force stimuli.<sup>20</sup> These materials include mechanofluorochromic (MFC) and phosphorescent mechanochromic materials and may be widely used in sensors,<sup>21</sup> and security inks.<sup>22</sup> Numerous kinds of organic molecules have been found to exhibit MFC behaviour, such as tetraphenylethene,<sup>23</sup> 9,10-divinylanthracene,<sup>24</sup> triphenylamine,<sup>25</sup> phenothiazine,<sup>26</sup> and  $\beta$ -diketone boron complexes,<sup>27</sup> and so on. However, the development of organic molecules with both MFC properties and sensing characteristics to gases remains a challenge.



**Scheme 1.** Molecular structure of **3C16PBBCP** with hydrogen bonding unit, proton-binding site and large cyano group.

In this study, we attempt to design a fluorescent organic molecule that can self-assemble into thin fibers, respond to acid vapor and exhibit MFC activity. The benzoxazole group is

<sup>a</sup> Tianjin Key Laboratory of Structure and Performance for Functional Molecules, Key Laboratory of Inorganic-Organic Hybrid Functional Material Chemistry, Ministry of Education, College of Chemistry, Tianjin Normal University, Tianjin, 300387, P.R. China. \*E-mail: xuepengchong@126.com

<sup>b</sup> College of Chemistry, Jilin University, 2699# Qianjin Street, Changchun, 130012, P. R. China.

† Footnotes relating to the title and/or authors should appear here.

Electronic Supplementary Information (ESI) available: [Absorption, fluorescence and NMR spectra of solution after adding TFA, IR spectra of as-synthesized and ground solids, and absorption and excitation spectra of solids and xerogel]. See DOI: 10.1039/x0xx00000x

confirmed to be excellent proton-binding unit and has been successfully used as building blocks to prepare sensors for pH and acid vapors.<sup>28</sup> Moreover, several studies verified that the cyano group with a large steric hindrance may suppress aggregation-caused quenching and promote molecule to possess MFC behavior.<sup>29</sup> In addition, the galunamide unit is a proven efficient functional group to induce the gelation and self-assembly of molecule and solvents into one-dimensional nanofibers.<sup>30</sup> Therefore, a galunamide derivative consisting of a fluorophore with cyano and benzoxazole moieties was designed and synthesized. This compound can gelate certain solvents and self-assemble into one-dimensional nanofibers with strong yellow fluorescence. The nanofibers could respond to acids not only in solution but also in gel phase. Interestingly, the xerogel film also emitted strong fluorescence, which can be quenched by volatile acid vapors. The detection limit for trifluoroacetic acid (TFA) reaches 70 ppb. As expected, mechanical force stimulus can induce fluorescence change from green to orange. Moreover, solvent annealing leads to fluorescence recovery, showing a reversible MFC behavior.

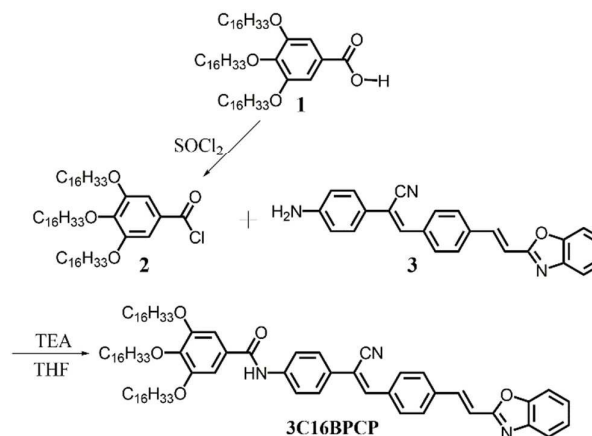
## Experiment section

**Measurements and instruments:** <sup>1</sup>H NMR and <sup>13</sup>C NMR spectra were recorded using a Mercury Plus instrument at 400 MHz and 100 MHz in CDCl<sub>3</sub> in all cases. FT-IR spectra were recorded using a Nicolet-360 FT-IR spectrometer by incorporation of samples into KBr disks or casting sample in a NaCl crystal. UV-vis spectra were obtained on a Mapada UV-1800pc spectrophotometer. Fluorescence emission spectra were obtained on a Cary Eclipse fluorescence spectrophotometer. C, H, and N elemental analyses were performed on a PerkinElmer 240C elemental analyzer. Mass spectra were obtained with AXIMA CFR MALDI-TOF (Compact) mass spectrometer. Transmission electron microscopy (TEM) images were observed with a Hitachi H-8100 apparatus by wiping the samples onto a 200-mesh carbon coated copper grid followed by naturally evaporating the solvent. Scanning electron microscopy (SEM) was performed on HITACHI SU8020 (operating at 3.0 kV). The samples were prepared by casting the wet gels onto a clean silicon wafer followed by drying in air. Before observation, the samples were coated by a gold film. Fluorescence microscopy (FM) images were obtained on fluorescence microscope (Olympus Reflected Fluorescence System BX51, Olympus, Japan).

**Gelation Ability Investigation:** The solution containing 5.0 mg gelator in selected organic solvent (1.0 mL) was heated in a sealed bottle with 1 cm diameter by a heating panel until the solid was dissolved. After the solution was cooled to room temperature and placed for 6 h, the gel state was evaluated by the "stable to inversion of a test tube" method.

**Preparation and measurement of sensing film: 3C16BPCP** (1.0 mg) was dissolved in DMSO (1.5 mL) under heating to form clear solution at 160 °C. A hot solution of 10.0 μL was casted uniformly on the glass slide (1.0 × 2.5 cm) at 90 °C, and then the sample was aged at room temperature until a gel film was formed. After 2 h, the solvent was removed in a vacuum oven.

The glass slide was placed in a cell (optical path = 1 cm) and the cell was sealed by sealing film. The gaseous acids at different concentrations were simply obtained by injecting saturated vapor with certain volume into the cell. Then, the fluorescence of xerogel film was measured after 5 min. Synthesis, procedures, and characterization



Scheme 2. Synthesis route of 3C16BPCP.

3C16BPCP was easily obtained by a one-step reaction from 1 and 2 in the presence of triethylamine, as shown in Scheme 2. Compounds 1 and 3 were synthesized by the reported methods.<sup>31,32</sup> The detailed experimental procedure was as follows:

### N-(4-((Z)-2-(4-((E)-2-(benzo[d]oxazol-2-yl)vinyl)phenyl)-1-cyanovinyl)phenyl)-3,4,5-tris(hexadecyloxy)benzamide (3C16BPCP)

1 (2.0 g, 2.37 mmol) was dissolved in SOCl<sub>2</sub> (5 mL) and the mixture was refluxed for 5 h. After removing the excess SOCl<sub>2</sub> corresponding acyl chloride 2 was obtained and used without further purification. 2 was dissolved in dry CH<sub>2</sub>Cl<sub>2</sub> (20 mL) with triethylamine (0.66 mL). The mixture was cooled in an ice-water bath. The THF solution of 3 (0.86 g, 2.37 mmol) was added dropwise and then the mixture was stirred for 12 h at room temperature. Water was added and then organic layer was separated and dried over Na<sub>2</sub>SO<sub>4</sub>. After the solvent was removed, the residue was purified by column chromatography using petroleum ether/CH<sub>2</sub>Cl<sub>2</sub> (v/v = 1/2) as an eluent. Yellow solid was obtained in a yield of 82%. <sup>1</sup>H NMR (400 MHz, CDCl<sub>3</sub>) δ 7.97 (d, J = 8.4 Hz, 2H), 7.85 (d, J = 16.4 Hz, 1H), 7.84 (s, 1H), 7.79 – 7.74 (m, 3H), 7.71 (m, 4H), 7.60 – 7.54 (m, 1H), 7.53 (s, 1H), 7.42 – 7.32 (m, 2H), 7.19 (d, J = 16.3 Hz, 1H), 7.06 (s, 2H), 4.13 – 3.96 (m, 6H), 1.90–1.26 (m, 84H), 0.88 (t, J = 6.7 Hz, 9H) (Fig. S9). <sup>13</sup>C NMR (101 MHz, CDCl<sub>3</sub>) δ 165.70, 162.44, 153.30, 150.47, 142.15, 141.81, 139.89, 139.24, 138.13, 137.00, 134.91, 130.06, 129.82, 129.41, 128.01, 126.79, 125.53, 124.68, 120.37, 120.01, 117.92, 115.41, 111.57, 110.42, 105.91, 73.61, 69.52, 31.94, 30.36, 29.74, 29.68, 29.61, 29.44, 29.39, 26.11, 22.71, 14.13 (Fig. S10).

MALDI-TOF MS: m/z: calcd: 1187.9; found: 1187.7 M<sup>+</sup> (Fig. S11). Chemical Formula: C<sub>79</sub>H<sub>117</sub>N<sub>3</sub>O<sub>5</sub> Elemental Analysis: C, 79.82; H, 9.92; N, 3.53; O, 6.73. FT-IR (KBr, cm<sup>-1</sup>): 3280, 2915, 2850, 2213, 1655, 1578, 1520, 1492, 1467, 1342, 1120.

## Results and discussion

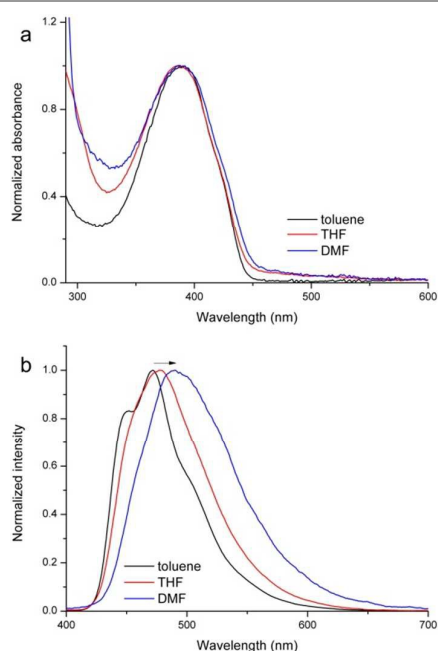


Fig. 1 Absorption and emission spectra of **3C16BPCP** in different solvents.  $\lambda_{\text{exc}} = 380$  nm.

## Photophysical properties in solution.

The absorption and emission spectra of **3C16BPCP** were first investigated. As shown in Fig. 1, the maximal absorption peak is located at 388 nm in toluene. The absorption spectra in THF and DMF with large polarities are similar to that in toluene. The maximal fluorescence peak in toluene is located at 471 nm with two shoulder peaks at 450 and 500 nm, implying a vibrational structure. The shoulder peaks disappear, and the emission bands broaden in polar solvent. Moreover, the maximal emission peaks show a bathochromic shift. For example, the THF solution presents a maximal emission peak at 478 nm that further shifts to 490 nm in DMF. These spectral changes suggest that **3C16BPCP** in the excited state bears a larger polarity relative to that in ground state because of the molecular weak donor–acceptor characteristics.<sup>33</sup>

Owing to the existence of the benzoxazole unit, the **3C16BPCP** solution is expected to respond to acids. As shown in Fig. S1, the absorption peak is located at 382 nm, which gradually decreases after TFA addition. Simultaneously, the absorbance at ca. 450 nm increases upon the application of TFA stimulus. Moreover, the addition of TFA results in changes in the emission spectra. The emission peak at 472 nm becomes weak upon the addition of 2.0 equiv. TFA, and the intensity around 500–600 nm increases. With further addition of TFA, the peak at 472 nm gradually disappears, and a new peak at ca. 530 nm appears. These results indicate that **3C16BPCP** responds to acid in solution. NMR spectra were used to further understand the interaction between **3C16BPCP** and the acid. Evident downfield shifts were observed for three vinyl group upon the addition of TFA (Fig S2b), suggesting that electron densities around these protons decrease upon the addition of

TFA. Based on the absorption, emission and NMR spectra, the response of **3C16BPCP** to TFA is due to the binding of benzoxazole unit to proton (Fig. S2a).<sup>34</sup>

## Self-assembly in gel.

Table 1. Gelation ability of **3C16BPCP** in organic solvents.<sup>a</sup>

Solvent	Status (CGC) <sup>b</sup>	Solvent	Status (CGC)
Cyclohexane	P	THF	S
<i>n</i> -Hexane	P	Ethyl acetate	G (0.84)
<i>n</i> -Octane	P	Acetone	G (0.56)
Toluene	S	Acetophenone	G (2.1)
<i>o</i> -Dichlorobenzene	S	3-Pentanone	G (4.2)
CHCl <sub>3</sub>	S	Acetic acid	G (0.84)
Ethanol	I	DMSO	G (0.21)
CH <sub>2</sub> Cl <sub>2</sub>	S	DMF	G (0.70)

<sup>a</sup> G: gel; I: insoluble; S: soluble; P: precipitate; <sup>b</sup> critical gelation concentration (mmol/L).

First, the gelation ability in different solvents was investigated, and the results are listed in Table 1. The gel could dissolve in nonpolar solvents, such as cyclohexane, *n*-hexane, and *n*-octane, under heating, but only yellow precipitate appears when the hot solutions were cooled to room temperature. **3C16BPCP** is highly soluble in aromatic solvents (toluene and *o*-dichlorobenzene), CH<sub>2</sub>Cl<sub>2</sub>, and THF. However, **3C16BPCP** forms yellow gels in certain organic solvents, such as ethyl acetate, acetone, acetophenone, 3-pentanone, acetic acid, DMSO, and DMF. Moreover, certain solvents possess low critical gelation concentrations. A 1.0 mg portion of **3C16BPCP** can gelate 4.0 mL DMSO, corresponding to  $2.1 \times 10^{-4}$  mol/L. That is, one gelator may prevent more than 67000 DMSO molecules from flowing. This result shows that **3C16BPCP** is an excellent gelator for certain solvents.

Thereafter, the self-assembly of **3C16BPCP** was investigated by SEM, TEM, FM, IR, and absorption and emission spectra. Fig. 2 shows SEM, TEM and FM images. From the SEM and TEM images, we can find that the DMSO gel was composed by numerous long, thin fibers with diameters of 50–200 nm. The small diameter provides large surface area, which favors the adsorption of analytes and decreases detection limit. The FM image of DMSO gel shows that gel fibers emit bright yellow fluorescence (Fig. 2c) when excited by the light at 330–385 nm, and numerous fibers construct a 3D network. The results show that gelators form one-dimensional self-assemblies in gel phase with the help of the intermolecular non-covalent interaction. Then, IR, absorption, and emission spectra were used to study the driving force of molecular self-assembly.

In the IR spectrum of xerogel, the vibration peak of C=O group is located at  $1666 \text{ cm}^{-1}$ . A wide and weak peak at  $3287 \text{ cm}^{-1}$  corresponding to the vibration of N-H is also found, which suggests a weak intermolecular hydrogen bond between aromatic amide groups.<sup>35</sup> In addition, two strong vibration peaks at 2918 and  $2850 \text{ cm}^{-1}$  ascribed to long alky chains ((CH<sub>2</sub>)<sub>n</sub>) indicates the existence of van der Waals interactions of aliphatic alkyl chains.<sup>36</sup>

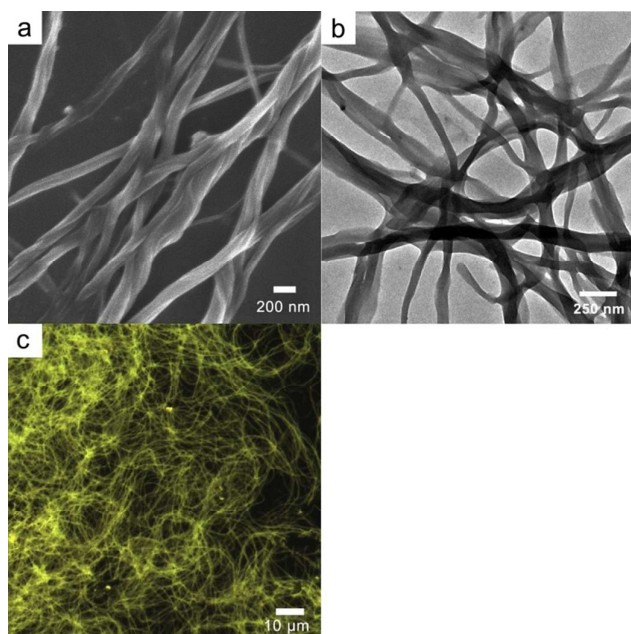


Fig. 2 (a) SEM, (b) TEM and (c) FM images of 3C16BPDP DMSO gel.

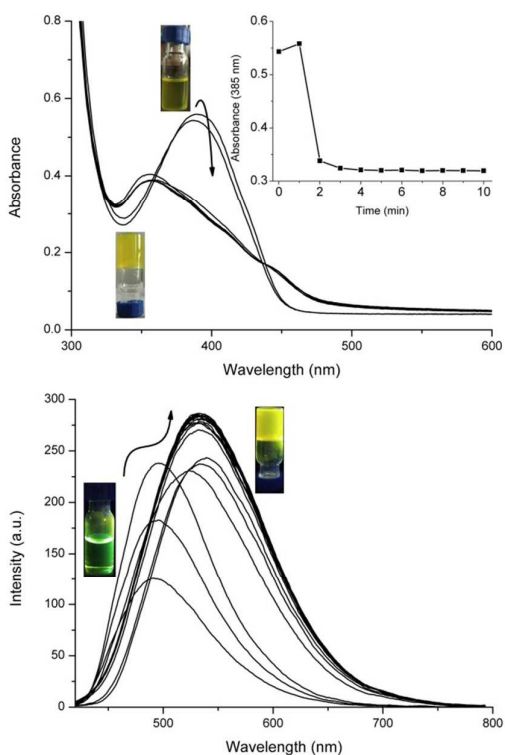


Fig. 3 (a) Absorption and (b) fluorescence spectral change during gelation from 180 to 20 °C. Concentration is 0.5 mg/mL,  $\lambda_{ex}$ =380 nm. Insets in Fig. 3a are the photos of sol and gel and the change of absorbance at 385 nm during gelation, and insets in Fig. 3b are the photos of sol and gel under 365 nm.

Absorption and emission spectra were utilized to study  $\pi$ - $\pi$  interaction between aromatic moieties during gelation. As shown in Fig. 3a, the maximal absorption peak appears at 386 nm in DMSO at 180 °C. This absorption peak increases and

shifts to 389 nm after cooling for 1 min probably because of molecular planarization. After 2 min, this peak almost disappears, and a new absorption peak at 356 nm appears owing to molecular aggregation and the formation of H-aggregates.<sup>37</sup> Gelation also results into fluorescence spectral change. The hot solution emits green fluorescence, but yellow fluorescence is observed for DMSO gel (Fig. 3b). During gelation, the maximal emission peak at 490 nm first arises and then exhibits a red shift to 530 nm. As a result, a gel can emit enhanced fluorescence. These spectral changes illustrate strong exciton interaction between aromatic groups, which may actually be beneficial to amplify the signal of analytes owing to exciton diffusion. In addition, we found that the gel in acetic acid emits weak orange fluorescence. During gelation, the hot solution exhibits yellow fluorescence with a maximum at 475 nm; however, this peak almost disappears, and a peak at 581 nm emerges in the gel phase (Fig. S4). This finding indicates that the fluorescence of the gel fibers may respond to acid stimuli. Next, the responsive property of xerogel film to acid vapor will be investigated.

Moreover, XRD pattern of DMSO gel was obtained to understand the molecular packing in gel phase. As shown in Fig. S5a, there are several wide diffraction peaks from 5° to 30°, suggesting the ordering in gel phase is poor.

#### Response of xerogel film to acid vapour.

Xerogel films were easily prepared by casting of hot solution on the glass plate followed by solvent evaporation. The xerogel film possesses strong yellow fluorescence, which could rapidly be quenched by TFA vapor and emit orange fluorescence (Fig. 4a, inset). Then, fluorescence spectra were used to investigate the relation between fluorescence intensity and TFA vapor concentration. As shown in Fig 4a, the maximal emission peak is located at 553 nm. A continuous decrease in emission intensity and a gradual red shift in emission peak were observed with increasing TFA concentration. When the concentration of TFA reaches 384 ppm, the emission peak shows a maximum at 594 nm rooted in the gelator bound with proton. The concentration-dependent fluorescence quenching efficiency (QE,  $1-I/I_0$ ) was plotted to demonstrate the sensitivity of the xerogel film for sensing gaseous TFA in Fig. 4b. The QE is saturated at TFA vapor concentrations exceeding 256 ppm. Moreover, a noticeable quenching of 44% in the fluorescence emission can be observed by the TFA vapor of 32 ppm. A detection limit of the xerogel film is determined as 70 ppb for the TFA vapor. Moreover, the sensing property of xerogel film to acetic acid vapor as weak acid was studied (Fig. S6). The fluorescence of xerogel film possesses lower sensitivity to acetic acid than that to TFA. An acetic acid concentration of 240 ppm only induces a QE of 5.6 % probably because the weak acidity of acetic acid induces gelator can hardly be protonated. To further clarify the distinct response of gel film to TFA and acetic acid, we checked the  $pK_b$  of gelator as base by measuring absorption spectra in different pH solutions. It is 11.3, implying that the  $pK_a$  of its conjugated acid is 2.7. Because  $pK_a$ s of TFA and acetic acid are 0.23 and 4.76, TFA can protonate gelator, but acetic acid cannot do it.

Therefore, the gel film exhibited poor sensitivity to acetic acid vapor. Thus, our xerogel film may act a sensing material to quantitatively detect TFA vapor.

#### Mechanofluorochromism of 3C16BPCP in solid state.

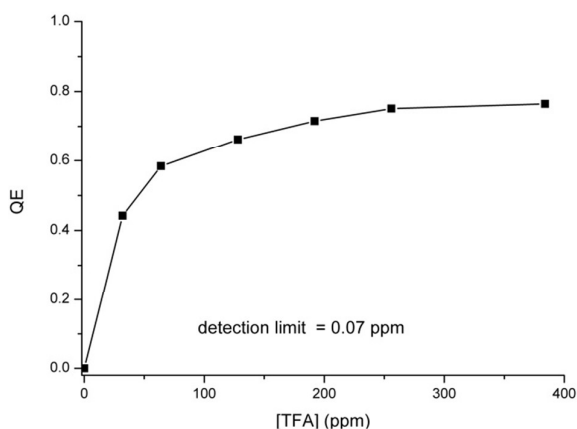
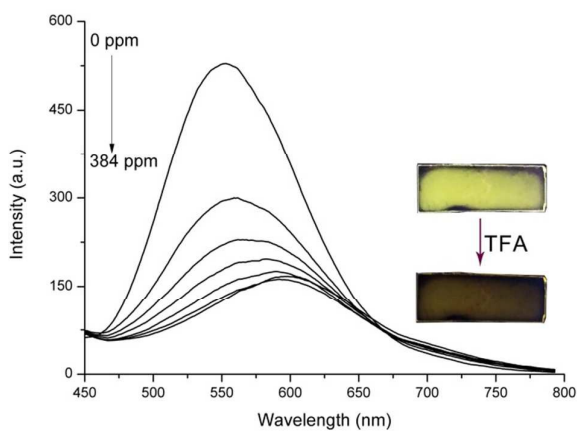


**Fig. 4** (a) Changes in the spectral emission of the xerogel film exposed to different concentrations of TFA vapours for 10 s. (b) Concentration-dependent fluorescence QE of the film. The intensity was monitored at 525 nm.

We found that the as-synthesized solid from THF emitted green fluorescence and fluorescence color changed into orange when lightly pressed, indicating mechanofluorochromism.<sup>38</sup> Thereafter, the fluorescence spectra were utilized to monitor MFC behavior of 3C16BPCP in the solid state. As shown in Fig. 5a, a maximal emission peak at 510 nm appears in as-synthesized solid, allowing it to have green fluorescence with light irradiated at 365 nm. The ground powder emitted orange fluorescence centered at 550 nm. When ground solid was exposed to gaseous common solvents, such as  $\text{CH}_2\text{Cl}_2$ , THF, toluene, DMSO, and DMF, fluorescence color was not recovered. Moreover, thermal annealing did not induce the recovery of the fluorescence spectrum. However, green fluorescence reappeared and fluorescence spectrum was consistent with that of as-synthesized solid when a drop of  $\text{CH}_2\text{Cl}_2$  was added to the surface of ground powder (Fig. 5a). In addition, the addition of other solvents, such as THF, toluene and cyclohexane could result in green fluorescence recovering, implying that recrystallization in the help of solvents should be responsible for fluorescence restoration.

Furthermore, restoration of the solid with green fluorescence by grinding will result in a fluorescence color change from green to orange. This fluorescence color switch could be repeatedly observed by grinding and then solvent annealing. These results show that the MFC behavior of 3C16BPCP is reversible (Fig 5a, inset).<sup>39</sup>

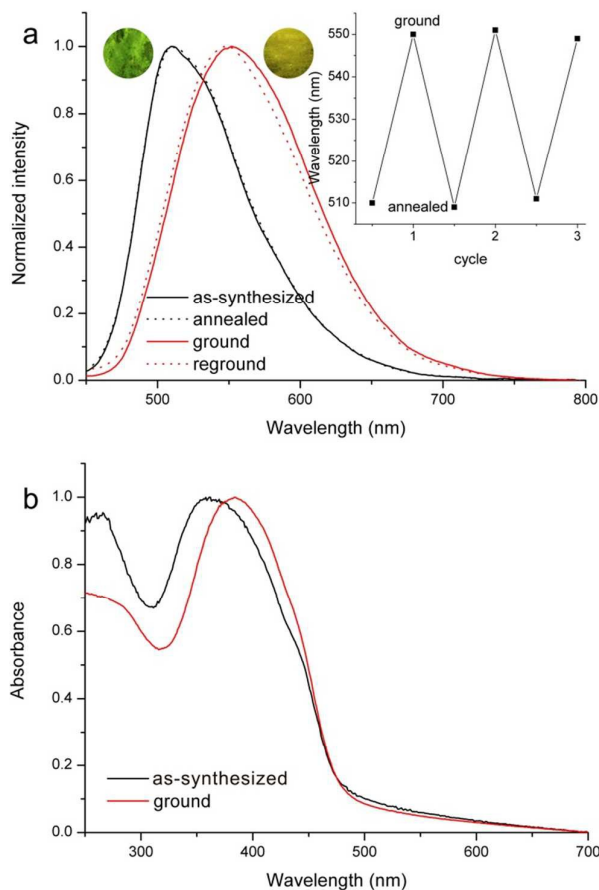


**Fig. 5** (a) Normalized fluorescence spectra of 3C16BPCP in the solid state under external stimuli. Inset: photos under 365 nm light.  $\lambda_{\text{ex}} = 400$  nm.

For an insight into the MFC mechanism, absorption, excitation, and IR spectra were conducted on the as-synthesized and ground material. As shown in Fig. 5b, the maximal absorption peak emerges at 360 nm, which is similar to that in the gel phase, suggesting that face-to-face H-aggregates exist in the as-synthesized solid. However, the emission spectrum of as-synthesized solid is at 510 nm, which is shorter than that of xerogel (553 nm). XRD pattern of as-synthesized solid was obtained to understand the emission difference. As-synthesized solid has strong and sharp diffraction peaks in small and wide angle region and these diffraction peaks are different from those of gel (Fig. 55b), indicating that a different packing model from that in gel and more ordered packing in as-synthesized solid relative to in gel. This result illustrates that different molecular stacking result in their distinct emission wavelength. When the as-synthesized solid was ground for 2 min, the absorption peak emerged at 384 nm, which shows a slight blue shift relative to that in toluene solution (388 nm).

This finding suggests that mechanical force stimulus leads to the disappearance of H-aggregates. Then, the excitation spectra before and after grinding were compared (Fig. S7). The maximal excitation peak of as-synthesized solid is located at 355 nm, which is similar to that in its absorption spectrum (360 nm). This excitation peak becomes weak while the solid is being ground, indicating that some H-aggregates were broken. This result is in good agreement with those obtained by absorption spectral change.

Fig. S8 shows the IR spectra of **3C16BPCP** solid before and after mechanical force stimulus. As the as-synthesized solid presents two sharp vibration peaks at 3276 and 1655  $\text{cm}^{-1}$ , which are ascribed to N-H and C=O stretching vibrations and indicate the existence of intermolecular hydrogen bonds between amide groups in the as-synthesized solid. However, grinding of the solid induces the weakening of primal two peaks and the emergence of two new peaks at 3385 and 1679  $\text{cm}^{-1}$ . Given that the stronger hydrogen bonds are correlated with lower wavenumber shift of N-H and C=O stretching vibration peaks, the IR spectral change clearly illuminates that mechanical force partially destroys hydrogen bonds between amide moieties.<sup>40</sup> XRD pattern of ground solid was also measured. It was found that ground solid had weaker diffraction peaks relative to as-synthesized solid, implying grinding destroyed molecular stacking ordering.

Based on the above observations, a brief MFC mechanism for **3C16BPCP** is given as follows (Fig. 6). In as-synthesized solid, hydrogen bonds between amide groups and H-aggregate exist. However, poor stacking order between fluorophores promotes short emission wavelength. After grinding, hydrogen bonds and H-aggregate are destroyed, but the distance between fluorophores becomes short owing to the mechanical force stimuli, and then ground solid emits longer wavelength fluorescence. After treatment by solvent, hydrogen bonds and H-aggregates form again, and fluorescence is recovered.

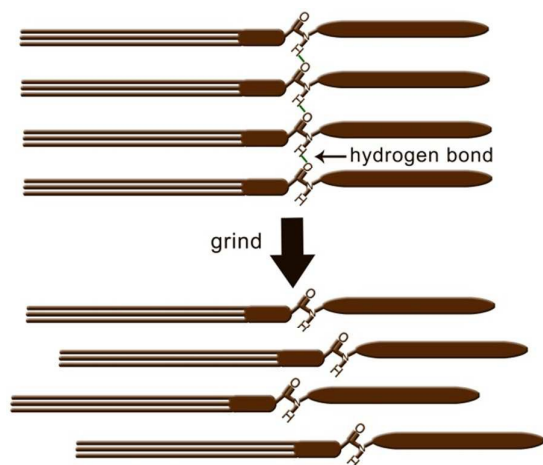


Fig. 6 Mechanofluorochromic mechanism of **3C16BPCP** in solid.

## Conclusions

A fluorescent gelator with cyano and benzoxazole moieties was synthesized. The gelator could form gels in certain solvents and self-assemble into nanofibers in the gel phase. The spectral investigations suggest that the driving forces of gel formation are the hydrogen bonds between amide groups,  $\pi$ - $\pi$  interaction between aromatic moieties, and van der Waals interactions of aliphatic alkyl chains. Moreover, the fluorescence of the xerogel film could be quenched, and the fluorescence color changed from yellow to orange-red upon exposure to TFA vapor, and a low detection limit of 70 ppb was achieved. More interestingly, mechanical force grinding led to fluorescence color change from green to orange because intermolecular hydrogen bonds and pristine  $\pi$ - $\pi$  interaction was destroyed by mechanical force. As a result, this molecule possesses dual responses to acid vapor and mechanical force. This implies that rational structure design may make molecules possess multiple responses to external stimuli.

## Acknowledgements

This work was financially supported by the National Natural Science Foundation of China (21103067), the Youth Science Foundation of Jilin Province (20130522134JH), the Open Project of State Laboratory of Theoretical and Computational Chemistry (K2013-02).

## Notes and references

- (a) Z. Qiu, H. Yu, J. Li, Y. Wang and Y. Zhan, *Chem. Commun.*, 2009, 3342; (b) X. Xiao, J. Hu, X. Gui and K. Qian, *Polymers* 2017, **9**, 87; (c) T. A. Barendt, S. W. Robinson and P. D. Bee, *Chem. Sci.*, 2016, **7**, 5171; (d) E. R. Kay, D. A. Leigh and F. Zerbetto, *Angew. Chem., Int. Ed.*, 2007, **46**, 72; (e) Y. Zhang, J. Yu, H. N. Bomba, Y. Zhu, and Z. Gu, *Chem. Rev.*, 2016, **116**, 12536; (f) Y. Zang, F. Zhang, D. Huang, X. Gao, C. Di and D. Zhu, *Nat. Commun.* 2015, **6**, 6269.
- (a) H. S. Jung, P. S. Kwon, J. W. Lee, J. I. Kim, C. S. Hong, J. W. Kim, S. Yan, J. Y. Lee, J. H. Lee, T. Joo and J. S. Kim, *J. Am. Chem. Soc.*, 2009, **131**, 2008; (b) Hyo Sung Jung, Peter Verwilt, W. Y. Kim and J. S. Kim, *Chem. Soc. Rev.*, 2016, **45**, 1242; (c) L. He, B. Dong, Y. Liu and W. Lin, *Chem. Soc. Rev.*, 2016, **45**, 6449; (d) K. Y. Zhang, X. Chen, G. Sun, T. Zhang, S. Liu, Q. Zhao and W. Huang, *Adv. Mater.*, 2016, **28**, 7137; (e) H. Shi, H. Sun, H. Yang, S. Liu, G. Jenkins, W. Feng, F. Li, Q. Zhao, B. Liu and W. Huang, *Adv. Funct. Mater.*, 2013, **23**, 3268; (f) W. Lin, Q. Zhao, H. Sun, K. Y. Zhang, H. Yang, Q. Yu, X. Zhou, S. Guo, S. Liu and W. Huang, *Adv. Opt. Mater.*, 2015, **3**, 368; (g) H. Sun, S. Liu, W. Lin, K. Y. Zhang, W. Lv, X. Huang, F. Huo, H. Yang, G. Jenkins, Q. Zhao and Wei Huang, *Nat. Commun.*, 2014, **5**, 3601.
- (a) Z. Guo, S. Park, J. Yoon and I. Shin, *Chem. Soc. Rev.*, 2014, **43**, 16; (b) M. H. Lee, J. S. Kim and J. L. Sessler, *Chem. Soc. Rev.*, 2015, **44**, 4185.
- Y. E. X. Ma, Y. Zhang, Y. Zhang, R. Duan, H. Ji, J. Li, Y. Che and J. Zhao, *Chem. Commun.* 2014, 50, 13596.
- R. Xu, Y. Wang, X. Duan, K. Lu, D. Micheroni, A. Hu and W. Lin, *J. Am. Chem. Soc.*, 2016, **138**, 2158.
- H. Yuan, Y. Fan, C. Xing, R. Niu, R. Chai, Y. Zhan, J. Qi, H. An and J. Xu, *Anal. Chem.*, 2016, **88**, 6593.

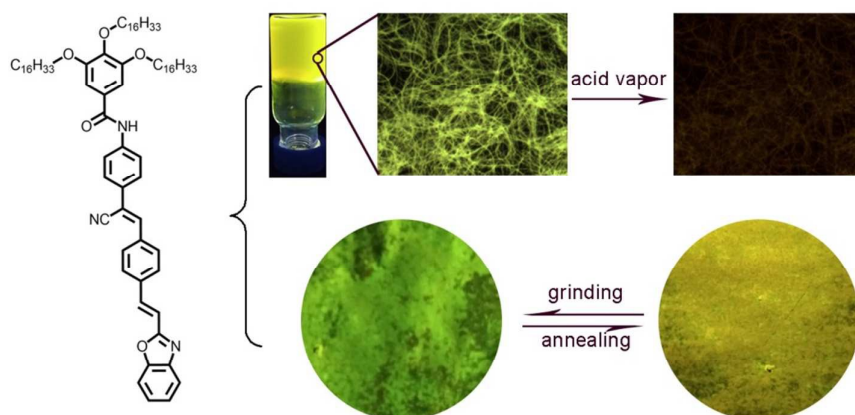
- 7 S. Che, R. Dao, W. Zhang, X. Lv, H. Li and C. Wang, *Chem. Commun.*, 2017, **53**, 3862.
- 8 X. Li, C. Wang, Y. Wan, W. Lai, L. Zhao, M. Yin and W. Huang, *Chem. Commun.*, 2016, **52**, 2748.
- 9 M. Strobl, A. Walcher, T. Mayr, I. Klimant, and S. M. Borisov, *Anal. Chem.*, 2017, **89**, 2859.
- 10 H. Zhang, W. B. Euler, *Sensor and Actuat. B-Chem.* 2016, **225**, 553.
- 11 Honglae Sohn, R. M. Calhoun, M. J. Sailor, W. C. Trogler, *Angew Chem. Int. Ed.* 2001, **40**, 2104.
- 12 Y. Hu, X. Ma, Y. Zhang, Y. Che and J. Zhao, *ACS Sens.* 2016, **1**, 22.
- 13 (a) P. Terech and R. G. Weiss, *Chem. Rev.* 1997, **97**, 3133; (b) Z. Zhao, J. W. Y. Lam, B. Z. Tang, *Soft Matter* 2013, **9**, 4564; (c) S. S. Babu, V. K. Praveen and A. Ajayaghosh, *Chem. Rev.* 2014, **114**, 1973; (d) V. K. Praveen, C. Ranjith, E. Bandini, A. Ajayaghosh and N. Armaroli, *Chem. Soc. Rev.* 2014, **43**, 4222; (e) X. Yu, L. Chen, M. Zhang and T. Yi, *Chem. Soc. Rev.* 2014, **43**, 5346; (f) X. Z. Yan, F. Wang, B. Zheng and F. H. Huang, *Chem. Soc. Rev.* 2012, **41**, 6042; (g) Y. Feng, Y. He and Q. Fan, *Chem. Asian J.* 2014, **9**, 1724; (h) H. Chen, Y. Feng, G. Deng, Z. Liu, Y. He and Q. Fan, *Chem. Eur. J.* 2015, **21**, 11018; (i) Z. Sun, Q. Huang, T. He, Z. Li, Y. Zhang, and L. Yi, *ChemPhysChem* 2014, **15**, 2421.
- 14 Y. Che, X. Yang, S. Loser and L. Zang, *Nano Lett.*, 2008, **8**, 2219.
- 15 N. Velasco-García, M. J. Valencia-González and M. E. Díaz-García, *Analyst*, 1997, **122**, 1405.
- 16 (a) H. N. Peng, D. L. Ding, T. H. Liu, X. L. Chen, L. Li, S. W. Yin and Y. Fang, *Chem. -Asian J.* 2012, **7**, 1576; (b) X. Liu, X. Zhang, R. Lu, P. Xue, D. Xu, H. Zhou, *J. Mater. Chem.* 2011, **21**, 8756; (c) L. Zhai, M. Liu, P. Xue, J. Sun, P. Gong, Z. Zhang, J. Sun and R. Lu, *J. Mater. Chem. C* 2016, **4**, 7939; (d) P. Xue, Q. Xu, P. Qian, C. Gong, A. Ren, Y. Zhang and R. Lu, *Chem. Commun.* 2013, **49**, 5838; (e) S. Wang, P. Xue, P. Wang and B. Yao, *New J. Chem.* 2015, **39**, 6874; (f) J. Fan, X. Chang, M. He, C. Shang, G. Wang, S. Yin, H. Peng and Y. Fang, *ACS Appl. Mater. Interfaces* 2016, **8**, 18584
- 17 (a) P. Xue, J. Sun, B. Yao, P. Gong, Z. Zhang, C. Qian, Y. Zhang and R. Lu, *Chem. Eur. J.* 2015, **21**, 4712; (b) J. Peng, J. Sun, P. Gong, P. Xue, Z. Zhang, G. Zhang and R. Lu, *Chem. -Asian J.* 2015, **10**, 1717; (c) J. Sun, P. Xue, J. Sun, P. Gong, P. Wang, R. Lu, *J. Mater. Chem. C* 2015, **3**, 8888; (d) X. Cao, N. Zhao, G. Zou, A. Gao, Q. Ding, G. Zeng and Y. Wu, *Soft Matter*, 2017, **13**, 3802; (e) R. Li, S. Wang, Q. Li, H. Lan, S. Xiao, Y. Li, R. Tan and T. Yi, *Dyes Pigm.* 2016, **137**, 111.
- 18 (a) T. Naddo, Y. Che, W. Zhang, K. Balakrishnan, X. Yang, M. Yen, J. Zhao, J. S. Moore, and L. Zang, *J. Am. Chem. Soc.*, 2007, **129**, 6978; (b) K. K. Kartha, S. S. Babu, S. Srinivasan, A. Ajayaghosh, *J. Am. Chem. Soc.* 2012, **134**, 4834; (c) P. Gong, J. Sun, P. Xue, C. Qian, Z. Zhang, J. Sun and R. Lu, *Dyes Pigm.* 2015, **118**, 27; (d) N. Dey, S. K. Samanta and S. Bhattacharya, *ACS Appl. Mater. Interfaces*, 2013, **5**, 8394; (e) X. Cao, N. Zhao, H. Lv, Q. Ding, A. Gao, Q. Jing and T. Yi, *Langmuir*, 2017, **33**, 7788.
- 19 X. Yu, X. Ge, L. Geng, H. Lan, J. Ren, Y. Li, and T. Yi, *Langmuir*, 2017, **33**, 1090.
- 20 (a) Y. Sagara, S. Yamane, M. Mitani, C. Weder and T. Kato, *Adv. Mater.*, 2016, **28**, 1073; (b) Y. Jiang, *Mater. Sci. Eng., C*, 2014, **45**, 682; (c) Y. Q. Dong, J. W. Y. Lam and B. Z. Tang, *J. Phys. Chem. Lett.*, 2015, **6**, 3429; (d) Z. Chi, X. Zhang, B. Xu, X. Zhou, C. Ma, Y. Zhang, S. Liu and J. Xu, *Chem. Soc. Rev.*, 2012, **41**, 3878; (e) L. Bu, M. Sun, D. Zhang, W. Liu, Y. Wang, M. Zheng, S. Xue and W. J. Yang, *J. Mater. Chem. C*, 2013, **1**, 2028; (f) M. M. Caruso, D. A. Davis, Q. Shen, S. A. Odom, N. R. Sottos, S. R. White and J. S. Moore, *Chem. Rev.*, 2009, **109**, 5755; (g) A. P. Haehnel, Y. Sagara, Y. C. Simon and C. Weder, *Top. Curr. Chem.*, 2015, **369**, 345; (h) S. Xue, X. Qiu, Q. Sun and W. Yang, *J. Mater. Chem. C*, 2016, **4**, 1568; (i) Z. Ma, Z. Wang, M. Teng, Z. Xu and X. Jia, *ChemPhysChem*, 2015, **16**, 1811; (j) P. Xue, J. Ding, P. Wang and R. Lu, *J. Mater. Chem. C*, 2016, **4**, 6688; (k) Y. Ooyama and Y. Harima, *J. Mater. Chem.*, 2011, **21**, 8372.
- 21 Y. Wang, X. Tan, Y. Zhang, S. Zhu, I. Zhang, B. Yu, K. Wang, B. Yang, M. Li, B. Zou and S. X. Zhang, *J. Am. Chem. Soc.*, 2015, **137**, 931; (b) Y. Q. Dong, J. W. Y. Lam and B. Z. Tang, *J. Phys. Chem. Lett.*, 2015, **6**, 3429.
- 22 (a) Y. Wang, I. Zhang, B. Yu, X. Fang, X. Su, Y. Zhang, T. Zhang, B. Yang, M. Li and S. X. Zhang, *J. Mater. Chem. C*, 2015, **3**, 12328; (b) X. Zhu, R. Liu, Y. Li, H. Huang, Q. Wang, D. Wang, X. Zhu, S. Liu and H. Zhu, *Chem. Commun.*, 2014, **50**, 12951.
- 23 (a) H. Gao, D. Xu, X. Liu, A. Han, L. Zhou, C. Zhang, Z. Li, J. Dang, *Dyes Pigm.*, 2017, **139**, 157; (b) T. Jadhav, J. M. Choi, B. Dhokale, S. M. Mobin, J. Y. Lee, and R. Misra, *J. Phys. Chem. C*, 2016, **120**, 18487; (c) X. Zhang, Z. Chi, B. Xu, B. Chen, X. Zhou, Y. Zhang, S. Liu and J. Xu, *J. Mater. Chem.*, 2012, **22**, 18505.
- 24 K. Wang, H. Zhang, S. Chen, G. Yang, J. Zhang, W. Tian, Z. Su and Y. Wang, *Adv. Mater.*, 2014, **26**, 6168; Y. Dong, B. Xu, J. Zhang, X. Tan, L. Wang, J. Chen, H. Lv, S. Wen, B. Li, L. Ye, B. Zou and W. Tian, *Angew. Chem., Int. Ed.*, 2012, **51**, 10782; (c)
- 25 (a) Z. Zhang, Z. Wu, J. Sun, B. Yao, P. Xue and R. Lu, *J. Mater. Chem. C*, 2016, **4**, 2854; (b) P. Xue, P. Chen, J. Jia, Q. Xu, J. Sun, B. Yao, Z. Zhang and R. Lu, *Chem. Commun.*, 2014, **50**, 2569.
- 26 (a) P. Xue, B. Yao, X. Liu, J. Sun, P. Gong, Z. Zhang, C. Qian, Y. Zhang and R. Lu, *J. Mater. Chem. C*, 2015, **3**, 1018; (b) Y. Zhan, J. Zhao, P. Yang and W. Ye, *RSC Adv.*, 2016, **6**, 92144; (c) P. Xue, J. Ding, P. Chen, P. Wang, B. Yao, J. Sun, J. Sun and R. Lu, *J. Mater. Chem. C*, 2016, **4**, 5275.
- 27 (a) G. Zhang, J. P. Singer, S. E. Kooi, R. E. Evans, E. L. Thomas and C. L. Fraser, *J. Mater. Chem.*, 2011, **21**, 8295; (b) X. Cheng, D. Li, Z. Zhang, H. Zhang and Y. Wang, *Org. Lett.*, 2014, **16**, 880; (c) Y. Qi, Y. Wang, Y. Yu, Z. Liu, Y. Zhang, G. Du and Y. Qi, *RSC Adv.*, 2016, **6**, 33755.
- 28 (a) Y. Dong, J. Zhang, X. Tan, L. Wang, Ji. Chen, B. Li, L. Ye, B. Xu, B. Zou and W. Tian, *J. Mater. Chem. C*, 2013, **1**, 7554; (b) P. Xue, B. Yao, J. Sun, Z. Zhang, K. Li, B. Liu, Ran Lu, *Dyes Pigm.* 2015, **112**, 255.
- 29 (a) B. Wang, Y. Wang, J. Hua, Y. Jiang, J. Huang, S. Qian, H. Tian, *Chem. Eur. J.* 2011, **17**, 2647; (b) L. Zhou, D. Xu, H. Gao, A. Hana, Y. Yang, C. Zhang, X. Liu and F. Zhao, *RSC Adv.*, 2016, **6**, 69560; (c) B. An, S. Kwon, S. Jung, S. Y. Park, *J. Am. Chem. Soc.*, 2002, **124**, 14410.
- 30 (a) D. Pati, N. Kalva, S. Das, G. Kumaraswamy, S. S. Gupta and A. V. Ambade, *J. Am. Chem. Soc.*, 2012, **134**, 7796; (b) F. Camerel, R. Ziessel, B. Donnio, C. Bourgogne, D. Guillon, M. Schmutz, C. Iacovita and J. Bucher, *Angew. Chem. Int. Ed.*, 2007, **46**, 2659.
- 31 X. Qian, W. Gong, M. K. Dhinakaran, P. Gao, D. Na and G. Ning, *Soft Matter*, 2015, **11**, 9179.
- 32 P. Xue, B. Yao, P. Wang, P. Gong, Z. Zhang and Ran Lu, *Chem. Eur. J.*, 2015, **21**, 17508.
- 33 (a) Y. Zhang, K. Wang, G. Zhuang, Z. Xie, C. Zhang, F. Cao, G. Pan, H. Chen, B. Zou and Y. Ma, *Chem. Eur. J.* 2015, **21**, 2474; (b) C. Reichardt, *Chem. Rev.*, 1994, **94**, 2319.
- 34 P. Xue, R. Lu, J. Jia, M. Takafuji, and H. Ihara, *Chem. Eur. J.*, 2012, **18**, 3549.
- 35 (a) F. García and L. Sánchez, *J. Am. Chem. Soc.*, 2012, **134**, 734; (b) Y. Liu, C. Chen, T. Wang, and M. Liu, *Langmuir* 2016, **32**, 322; (c) S. Ray, M. Takafujia and H. Ihara, *Anal. Methods*, 2014, **6**, 7674.
- 36 (a) M. K. Nayak, B. Kim, J. E. Kwon, S. Park, J. Seo, J. Chung and S. Y. Park, *Chem. Eur. J.*, 2010, **16**, 7437; (b) M. M. Rahman, M. Czaun, M. Takafuji, and H. Ihara, *Chem. Eur. J.*, 2008, **14**, 1312.

## ARTICLE

Journal Name

- 37 (a) P. Ehrenreich, S. T. Birkhold, E. Zimmermann, H. Hu, K. Kim, J. Weickert, T. Pfadler and L. Schmidt-Mende, *Sci. Rep.*, 2016, **6**, 32434; (b) N. H. Mudliar and P. K. Singh, *Chem. Eur. J.*, 2016, **22**, 7394; (c) B. Lü, S. You, P. Li, C. Li, K. Müllen and M. Yin, *Chem. Eur. J.*, 2017, **23**, 397; (d) Z. Xie, V. Stepanenko, B. Fimmel and F. Würthner, *Mater. Horiz.*, 2014, **1**, 355.
- 38 Y. Sagara, A. Lavrenova, A. Crochet, Y. C. Simon, K. M. Fromm and C. Weder, *Chem. Eur. J.*, 2016, **22**, 4374.
- 39 (a) T. Han, X. Gu, J. W. Y. Lam, A. C. S. Leung, R. T. K. Kwok, T. Han, B. Tong, J. Shi, Y. Dong and B. Z. Tang, *J. Mater. Chem. C*, 2016, **4**, 10430; (b) B. Xu, Y. Mu, Z. Mao, Z. Xie, H. Wu, Y. Zhang, C. Jin, Z. Chi, S. Liu, J. Xu, Y. Wu, P. Lu, A. Lien and M. R. Bryce, *Chem. Sci.*, 2016, **7**, 2201; (c) S. Wan, Z. Ma, C. Chen, F. Li, F. Wang, X. Jia, W. Yang and M. Yin, *Adv. Funct. Mater.*, 2016, **26**, 353; (d) Z. Ma, Z. Wang, X. Meng, Z. Ma, Z. Xu, Y. Ma and X. Jia, *Angew. Chem., Int. Ed.*, 2016, **55**, 519; (e) S. Yagai, T. Seki, H. Aonuma, K. Kawaguchi, T. Karatsu, T. Okura, A. Sakon, H. Uekusa and H. Ito, *Chem. Mater.*, 2016, **28**, 234.
- 40 S. H. Cellman, G. P. Dado, C. Liang, and B. R. Adam, *J. Am. Chem. Soc.*, 1991, **113**, 1164.

## Graphic abstract



A galunamide derivative can quantitatively sense acid vapor in xerogel film state and change its fluorescence color under mechanical force stimuli.